

## Stability of Bubble Nuclei through Shell Effects

Klaus Dietrich and Krzysztof Pomorski\*

*Technische Universität München, Garching, Germany*

(Received 25 April 1997)

We investigate the shell structure of bubble nuclei in simple phenomenological shell models using Strutinsky's method. Shell energies down to  $-40$  MeV are shown to occur for certain magic nuclei. Estimates demonstrate that the calculated shell effects for certain magic numbers of constituents are probably large enough to produce stability against fission,  $\alpha$ , and  $\beta$  decay. No bubble solutions are found for mass number  $A \leq 450$ . [S0031-9007(97)05077-1]

PACS numbers: 21.10.Sf, 24.10.Nz, 47.20.Dr, 47.55.Dz

The possibility that nuclei could exist in the form of a (spherical) bubble or in the form of a toroid was pointed out long ago [1,2]. Within the liquid drop (LD) model, nuclei of these shapes turn out to be unstable with respect to deformations. Shell effects may, however, stabilize such nuclei against deformation.

In a series of papers, Wong [3] investigated shell effects for toroidal and bubble-shaped nuclei using Strutinsky's shell correction method. He restricted his attention to known nuclei near the valley of  $\beta$  stability and found that for certain doubly magic nuclei ( $^{200}_{80}\text{Hg}_{120}$ ,  $^{138}_{58}\text{Ce}_{80}$ ), spherical bubble solutions with a very small inner radius (ratio of inner to outer radius  $\approx 0.07$ ) turned out to be the ground state. Indications that bubble solutions might exist were also found in mean field calculations [4] and for stellar matter at finite temperature [5]. More recently, Moretto *et al.* [6] showed in a classical model that LD bubbles at finite temperature may be stabilized by an internal vapor pressure.

In the present paper, we study shell effects for nuclear bubbles in a broad range of neutron ( $N$ ) and proton ( $Z$ ) numbers extending considerably beyond the known nuclei. Bubble solutions for such nuclei were already found by Swiatecki [7] in the frame of the LD model and by Myers and Swiatecki [8] in the Thomas-Fermi model. Like Wong, we make use of Strutinsky's shell correction method [9]. We show that the shell energy may become as large as  $-40$  MeV for certain magic numbers of the nuclear constituents and that nuclear bubbles may thus become stable or very long lived against fission and other decay modes.

In Strutinsky's method [9], the total binding energy  $E$  of a nucleus (neutron number  $N$ , proton number  $Z$ , nucleon number  $A$ ) of a given shape is given as a sum of the liquid drop (LD) energy  $E_{\text{LD}}(N, Z)$  and the shell correction energy  $\delta E_{\text{shell}}$

$$E(N, Z) = E_{\text{LD}}(N, Z) + \delta E_{\text{shell}}(N, Z). \quad (1)$$

The shell correction energy has the well-known form [9].

We study the total energy, and especially the shell correction energy, of spherical nuclear bubbles. The single particle energies  $e_\nu$ , as well as the LD energy,

depend on the inner ( $R_2$ ) and outer ( $R_1$ ) radius of the bubble nucleus. Adopting the conventional saturation condition, the two radii are related by the equation,

$$R_1^3 - R_2^3 = R_0^3, \quad (2)$$

where  $R_0 = r_0 A^{1/3}$  is the radius of a compact spherical nucleus of the same mass. We describe the shape of the bubble nucleus by the ratio  $f$  between the volume of the hole and the volume of the entire bubble,

$$f := \frac{R_2^3}{R_1^3}. \quad (3)$$

Within the pure LD model, the energy of spherical bubble nuclei becomes smaller than the energy of a compact spherical nucleus for fissility parameters  $X_0 > 2.02$  (see Refs. [3,7]). These bubble solutions are not stable with respect to deformations [3] in the same way as the compact spherical liquid drops are not stable against fission for fissility parameters  $X_0 > 1$ . Nevertheless, stability can be produced by shell effects.

As two extreme and simple cases of nuclear single particle potentials, we considered the shell effects in an infinite square well and in a harmonic oscillator:

$$V(r) = \begin{cases} -V_0 & \text{for } R_2 < r < R_1 \\ +\infty & \text{otherwise} \end{cases}, \quad (4)$$

$$V(r) = -V_0 + \frac{M\omega^2}{2}(r - \bar{R})^2. \quad (5)$$

The depth  $V_0 > 0$  has no influence on the shell correction energy and can thus be put equal to zero. The center of the oscillator potential is chosen to be

$$\bar{R} = \frac{R_1 + R_2}{2}. \quad (6)$$

The oscillator frequency  $\omega$  is chosen in such a way that the rms deviation from the sphere of radius  $\bar{R}$  is the same when calculated with the shell model wave function and with the LD density

$$\langle (r - \bar{R})^2 \rangle_{\text{SM}} = \langle (r - \bar{R})^2 \rangle_{\text{LD}}. \quad (7)$$

We have to add a spin-orbit term to the central potential (4) or (5). We use the conventional form in the Skyrme approach [see Eq. (5.103) in Ref. [10]],

$$\hat{V}_{SO} = \tilde{V}_{SO}(r)\hat{\mathbf{l}} \cdot \hat{\mathbf{s}}, \quad (8)$$

$$\tilde{V}_{SO}(r) = \frac{3}{2} W_0 \frac{1}{r} \frac{\partial \rho(r)}{\partial r}, \quad (9)$$

where  $\rho(r)$  is the nuclear density distribution. We choose the value  $W_0 = 120 \text{ MeV fm}^5$  given in Ref. [10] and neglect the isospin dependence which is recently under debate [11].

For the total density  $\rho(r)$  which appears in the expression for the spin-orbit potential  $\tilde{V}_{SO}(r)$  [Eq. (9)], we used the following ansatz:

$$\rho(r) = \rho_0 \left[ 1 - 2 \left( \frac{r - \bar{R}}{R_1 - R_2} \right)^2 \right], \quad (10)$$

where  $\rho_0 = 0.17 \text{ fm}^{-3}$  and  $\bar{R}$  is given by Eq. (6). For simplicity we have assumed that the proton and neutron densities,  $\rho_p$  and  $\rho_n$ , are proportional to  $Z$  and  $N$ , respectively.

It is seen from (9) that the sign of the spin-orbit potential is opposite in the inner and outer surface region of the bubble nucleus. Consequently, the magnitude of the spin-orbit splitting is smaller for bubble nuclei than for normal ones. We, therefore, treat the spin-orbit term in perturbation theory. The eigenenergies  $e_{nlj}$  of the single particle (s.p.) Hamiltonian, including the spin-orbit potential (8) and the unperturbed eigenvalues  $\varepsilon_{nl}$ , are related by the equation

$$e_{nlj} = \varepsilon_{nl} + \langle \psi_{nljm} | \tilde{V}_{SO} | \psi_{nljm} \rangle \times [j(j+1) - l(l+1) - \frac{3}{4}], \quad (11)$$

where  $(n-1)$  represents the number of radial nodes (not counting zeros at  $r=0, \infty$ ) and  $l, j, m$  are the orbital and total angular momentum and its projection, respectively. The mean value  $\langle \psi_{nljm} | \tilde{V}_{SO} | \psi_{nljm} \rangle$  depends only on the unperturbed s.p. density

$$\rho_{nl}(r) = \psi_{nljm}^+(\mathbf{r})\psi_{nljm}(\mathbf{r}) = \frac{u_{nl}^2(r)}{r^2}. \quad (12)$$

The functions  $u_{nl}(r)$  satisfy the radial Schrödinger equation with eigenvalue  $\varepsilon_{nl}$ . For the infinite square well the

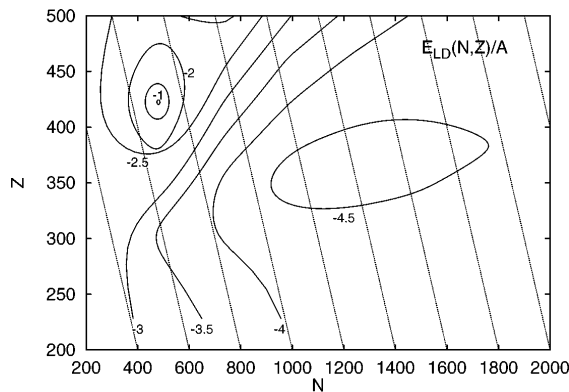


FIG. 1. Lines of constant LD binding energy per particle as a function of  $(N, Z)$ . Each point on the lines corresponds to a bubble solution within the LD model. The straight lines in the plot represent isobars.

eigenvalues and eigenfunctions are obtained by numerically satisfying the boundary conditions, and for the harmonic oscillator (5) we used the WKB approximation.

Results within the pure LD model are shown in Fig. 1. The LD parameters are taken from Ref. [12]. Each point on the equipotential lines corresponds to a spherical bubble solution as given by the LD model. It should be noted that the largest energy gains per particle occur for nucleon numbers  $1200 \leq A \leq 2000$  and the corresponding proton numbers  $325 \leq Z \leq 400$ . Some of the isobaric lines are cut twice by the same equienergy line. If the binding energy per particle in between these two points is smaller, a  $\beta$ -stable isobar lies somewhere on this section. Of course, this consideration is thwarted by the fact that the LD bubbles are all unstable against fission. In the LD model, the (spherical) bubble solutions are saddle points, not minima.

The LD results (and, consequently, also the result on the total binding energy) depend sensitively on the value of the surface constant  $\sigma$ .

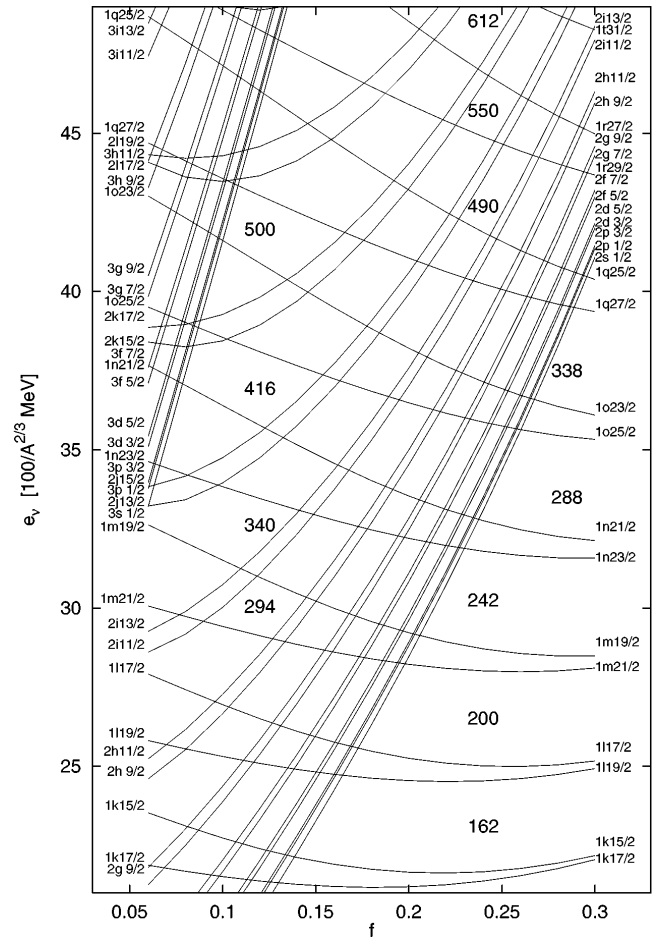


FIG. 2. Level scheme as a function of the hole fraction  $f = (R_2/R_1)^3$  for the infinite square well plus the spin orbit term [Eq. (4) and Eqs. (8)–(10)]. The energy unit used takes into account that the eigenvalues of the infinite square well scale with  $A^{-2/3}$ .

In Fig. 2 we show the spectrum of single particle levels for the shifted infinite square well with a spin-orbit term. The levels are shown as a function of the hole fraction parameter  $f$  [see Eq. (3)]. As  $f$  increases, the diameter  $d = R_1 - R_2$  of the bubble layer decreases. Increasing the number of radial nodes for given orbital angular momentum  $l$  thus costs an energy which rises steeply as a function of  $f$ . Augmenting a given  $l$  value by one for given  $n$  and given parameter  $f$  implies an increase in the centrifugal energy, which is larger, the larger the  $l$  value becomes. Magic numbers come about by the interplay between levels  $e_{nlj}$  with  $n \geq 2$ , which rise rapidly as a function of  $f$  and levels  $e_{1lj}$ , which depend more gently on  $f$  with a tendency to decrease with  $f$  due to the diminishing centrifugal energy. The level scheme for the harmonic oscillator has qualitatively very similar features.

For both potentials, we observe that the spin-orbit splitting is often reversed as compared to the case of normal nuclei. The reason was already given above. The shell correction energy  $\delta E_{\text{shell}}$  is shown as a function of  $N$  (or  $Z$ ) at a given value of  $f = 0.28$  for the infinite square well in Fig. 3. The eigenenergies of the square well scale with  $A^{-2/3}$  which is taken into account by the energy unit. It is seen from Fig. 3 that the shell energy may produce energy gains up to  $-20$  MeV for one sort of particles. Of course, double magic shell closures can only occur if the two magic numbers correspond to the same  $f$  values.

In Fig. 4 we display lines of equal energy gain by formation of a bubble. As a reference we use the energy of a spherical LD of the same number of neutrons and protons. It is seen that the gain in binding energy may amount to several 100 MeV.

We still have to deal with the crucial question of stability of the bubble solutions with respect to shape deformations. We describe the deformation dependence of the shell correction energy as suggested by Myers and Swiatecki [13]. In Fig. 5 we display the dramatic effect of the shell correction on the binding energy of a bubble nucleus as a function of the quadrupole deformation. The

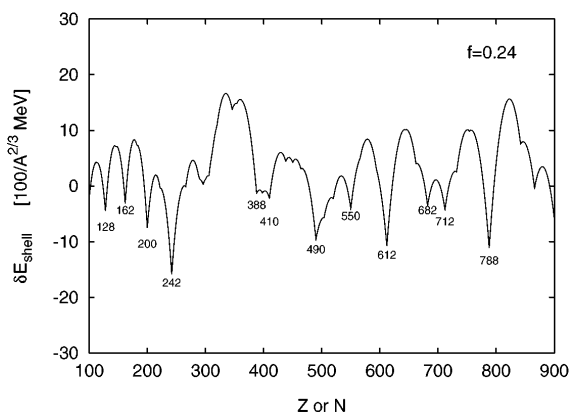


FIG. 3. Shell correction energy as a function of  $Z$  (or  $N$ ) for  $f = 0.28$  for the infinite square well.

total LD binding energy of the spherical bubble nucleus is put equal to zero. The LD part of the energy decreases monotonically as  $|\beta_2|$  increases. Adding the shell energy  $\delta E_{\text{shell}}$  with Swiatecki's  $\beta_2$  dependence produces a valley of about  $-30$  MeV depth. The barriers on both sides of the minimum are at about an energy of  $-3.9$  MeV which leaves us with a barrier height of about 25 MeV. This order of magnitude of the fission barrier implies an almost vanishing probability for spontaneous fission.

What about the other decay modes?  $\beta$  decay will imply that the system moves along isobaric lines in the  $(N, Z)$  plot, towards lower energy. Figure 1 is particularly instructive in this respect: If a given isobaric straight line cuts a line of constant binding energy twice and if, at the same time, the binding energy between the two points of intersection is lower, a  $\beta$ -stable nuclear bubble lies in between. In Fig. 1 this happens to be the case for  $A \geq 600$ . If, on the other hand, the energy keeps on lowering along a given isobaric direction, the  $\beta$  decays may finally lead to a nuclear composition where bubbles cease to exist. Thus there are cases where bubble nuclei may disintegrate by a series of  $\beta$  decays and others where the  $\beta$  decays make them approach a stable composition. Of course, the simple picture shown in Fig. 1 has a more complicated appearance when the shell correction energy is added.

The  $\alpha$  decay, which limits the lifetime of the presently known superheavy nuclei, certainly may also limit the lifetime of bubble nuclei. The penetrability of the Coulomb barrier for an  $\alpha$  particle depends exponentially on the Coulomb potential at  $r = R_1$ , which has the value  $2Ze_0/R_1$ . The higher the Coulomb potential, the lower the  $\alpha$ -decay probability. It can be found that, on the one hand, the typical energy of the outgoing  $\alpha$  particle is about 18 MeV as compared to about 5 MeV in the case of actinides, but, on the other hand, the effective potential barrier seen by the  $\alpha$  particle is higher by a few MeV than for typical actinide nuclei, due to the effect of

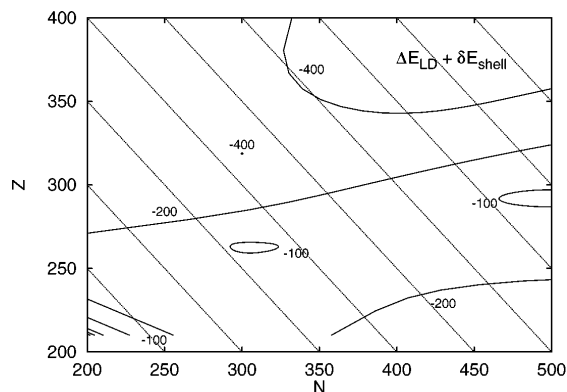


FIG. 4. Lines of constant energy gain ( $\Delta E_{\text{LD}} + \delta E_{\text{shell}}$ ) with respect to the energy of a compact spherical LD. The shell correction energy was calculated with the infinite square well potential.

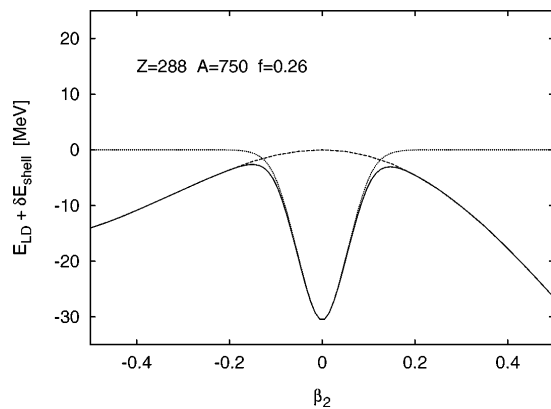


FIG. 5. LD energy (dashed line), shell correction energy (dotted line), and total energy (solid line) as a function of the quadrupole deformation  $\beta_2$  of the outer bubble surface  $S_1$ . The liquid drop energy was minimized with respect to the deformations  $\beta_4$  and  $\beta_6$  of the outer surface and  $\beta_2$  to  $\beta_6$  of the inner surface. The deformation dependence of the shell correction was taken from Ref. [13].

larger proton number  $Z$ . Consequently, the  $\alpha$  decay is not expected to be a mode of rapid decay.

It is intriguing to imagine that stable or at least very long-lived bubble nuclei may exist. Their properties would be a fascinating subject of research. Unfortunately, the masses and charges of the best candidates for bubble structure are so high that there is no hope to produce them. More careful work with the full Hartree-Bogoliubov theory is of course necessary, especially for determining the lower limits of mass and charge numbers of these objects. Even if bubble nuclei can never be made in a terrestrial laboratory, they might play a role in neutron stars [5].

Finally, there may be bubble structures for mesoscopic systems consisting of some 1000 atoms. This was already conjectured in Ref. [6]. We believe that it may also be

of interest to investigate whether shell effects favor the bubble topology for certain mesoscopic systems.

K.P. is grateful to the Deutsche Forschungsgemeinschaft (DFG) for financial support. Prior to 1 April 1997, this research was also supported by the Bundesminister für Bildung und Forschung (BMBF). This work was partially financed by the Polish Committee of Scientific Research under Contract No. 2P03B 049 09. K.D. is grateful for numerous stimulating discussions with M. Weiss.

\*On leave of absence from University M.C.S., Lublin, Poland.

- [1] P. J. Siemens and H. A. Bethe, Phys. Rev. Lett. **18**, 704 (1967).
- [2] J. A. Wheeler (unpublished).
- [3] C. Y. Wong, Ann. Phys. (N.Y.) **77**, 279 (1973) (with reference to earlier work).
- [4] P. Bonche, P. H. Heenen, and M. Weiss (private communication).
- [5] P. Bonche and D. Vauthérin, Nucl. Phys. **A372**, 496 (1981).
- [6] L. G. Moretto, K. Tso, and G. J. Wozniak, Phys. Rev. Lett. **78**, 824 (1997).
- [7] W. J. Swiatecki, Phys. Scr. **28**, 349 (1983).
- [8] W. D. Myers and W. J. Swiatecki, Nucl. Phys. **A601**, 141 (1996).
- [9] M. Brack, J. Damgaard, A. S. Jensen, H. C. Pauli, V. M. Strutinsky, and C. Y. Wong, Rev. Mod. Phys. **44**, 320 (1972).
- [10] P. Ring and P. Schuck, *The Nuclear Many Body Problem* (Springer-Verlag, New York, 1980).
- [11] P. G. Reinhard and H. Flocard, Nucl. Phys. **A584**, 467 (1995), and references therein.
- [12] W. D. Myers and W. J. Swiatecki, Ark. Fys. **36**, 343 (1966).
- [13] W. D. Myers and W. J. Swiatecki, Nucl. Phys. **81**, 1 (1966).